

The Potential of Chitosan Nanoparticles as a Delivery System for the Expression of Dengue Virus' rE Gene with pEGFP-N1 Vector in HeLa Cells

Muhammad Rizky Muzakki¹, Villa Sekar Cita¹, Nabilah Adzra Fahlevi¹, Tri Untari³, and Asmarani Kusumawati^{2*}

1. Master Program of Biotechnology, The Graduate School, Universitas Gadjah Mada, Yogyakarta 55281, Indonesia
2. Department of Reproduction, Obstetrics and Gynecology, Faculty of Veterinary Medicine, Universitas Gadjah Mada, Yogyakarta 55281, Indonesia
3. Department of Microbiology, Faculty of Veterinary Medicine, Universitas Gadjah Mada, Yogyakarta 55281, Indonesia

Article Info

Submitted: 08-10-2024

Revised: 12-05-2025

Accepted: 16-05-2025

*Corresponding author
Asmarani Kusumawati

Email:
uma_vet@ugm.ac.id

ABSTRACT

Dengue virus (DENV) infection is a global health concern, with severe cases primarily caused by antibody-dependent enhancement during secondary infections. The development of a multivalent vaccine providing balanced protection against all four DENV serotypes is therefore essential. One promising target is the recombinant envelope (rE) gene, which encodes a consensus E protein derived from the four DENV serotypes. Deoxyribonucleic acid (DNA) vaccine technology offers advantages such as induction of both humoral and cellular immune responses, scalable production, and storage stability; however, its efficacy is frequently limited by inefficient gene delivery. This study evaluated chitosan (CS) nanoparticles as a biocompatible, nontoxic delivery system for the rE gene. The pEGFP-N1-rE plasmid (N1-rE) was cloned into *Escherichia coli* DH5 α , with colony PCR, restriction analysis, and sequencing to confirm accurate insertion. N1-rE was complexed with CS nanoparticles at various DNA:CS mass ratios (w/w), with optimal complex formation at a 1:0.5 ratio, as confirmed via gel retardation assays. The N1-rE/CS complex demonstrated stability against DNase I and fetal bovine serum and exhibited low cytotoxicity with cell viability at 91.24%. The DNA-CS complex exhibited an average size of 217.4 nm, compatible with cellular uptake, and a zeta potential of -21.9 mV, suggesting moderate colloidal stability. Transfection analysis confirmed rE gene expression in HeLa cells. Quantitative PCR showed a 10.63-fold increase relative to controls, end-point RT-PCR detected a 134-bp amplicon, and confocal microscopy demonstrated enhanced cellular fluorescence (8.91×10^3 a.u.). These findings highlight the potential of CS nanoparticles as an effective delivery platform, laying the foundation for vaccine development strategies against DENV infection.

Keywords: chitosan; dengue virus; rE gene; gene delivery; HeLa cells

INTRODUCTION

Dengue is a mosquito-borne viral disease and a major global health burden, particularly in tropical regions. The disease is endemic in more than 100 countries, with Asia accounting for 70% of cases (World Health Organization, 2024). In Indonesia, 38,740 cases and 182 deaths were reported in 2025 up until April (Tarigan, 2025). Dengue virus (DENV) is primarily transmitted by

Aedes aegypti mosquitoes (Rahayu et al., 2019) and consists of four serotypes (DENV 1-4). While primary infection provides immunity to the same serotype, subsequent infection with a different serotype may induce severe disease through antibody-dependent enhancement (ADE) (Lai et al., 2019). Given the lack of antiviral therapies and reliance on supportive care (Asyura et al., 2021), prevention via vaccination is essential. However,

currently licensed dengue vaccines face limitations related to ADE and unbalanced immune responses. Dengvaxia increases the risk of severe dengue in seronegative individuals, whereas Qdenga provides strong protection against DENV-2 but has reduced efficacy against other serotypes (Halstead, 2024). These limitations highlight the urgent need for the development of safer, more broadly protective multivalent vaccines.

A promising vaccine target is the envelope (E) protein, which plays a key role in virus-host interactions (Alves et al., 2021). Fahimi et al. (2016) developed a recombinant E (*rE*) gene that combines the EDIII regions from all four DENV serotypes, resulting in a stable, immunogenic protein with the potential to elicit a balanced immune response. DNA vaccines appear to be an ideal platform for multivalent dengue antigen expression, as they can induce B and T cell responses and exhibit scalable production and storage stability (Srinivas, 2021). However, the development thereof remains hindered by their susceptibility to nuclease degradation and low cellular uptake (Srinivas, 2021). Chitosan, a biodegradable and biocompatible polymer that has been shown to protect DNA from nucleases and enhance cellular uptake, has the potential to be a safe delivery system for the DENV vaccine (Kaur et al., 2023; Santos-Carballal et al., 2018). Although earlier studies, such as that by Januar et al. (2019), have reported chitosan's effectiveness in delivering DNA for other viral genes; its capability for the delivery of the *rE* gene remains unexplored. This study was performed to evaluate the capability of chitosan nanoparticles to deliver and help enhance the expression of the *rE* gene in HeLa cells.

MATERIALS AND METHODS

The consensus *rE* gene derived from four DENV serotypes by Fahimi et al. (2016) was codon-optimized and synthesized into the pEGFP-N1 vector (pEGFP-N1-*rE*) by Gene Universal. Medium-molecular-weight chitosan (190–310 kDa, 85% deacetylation) (Sigma-Aldrich) was used as the DNA carrier. *Escherichia coli* DH5 α served as the cloning host, while HeLa cells from the Parasitology Laboratory, FK-KMK UGM, were used for transfection. Bacterial cultures were grown in Luria-Bertani (LB) medium containing bacteriological peptone (Oxoid), yeast extract (Oxoid), NaCl (Oxoid), agar (Oxoid) and kanamycin (Sigma).

Plasmid isolation was performed using the Plasmid DNA Extraction Maxi Kit (Favorgen Biotech Corp). Restriction enzyme digestion was performed using the *EcoRI* and *BglIII* enzymes with their respective reaction buffer (Invitrogen). RNA was extracted using the Quick-RNA Miniprep Kit (Zymo Research). Reverse transcription was performed with the ExcelRT™ Reverse Transcription Kit II (SMOBIO), PCR was performed using the PowerPol 2X PCR Mix (ABclonal), and qPCR was performed with the ExcelTaq™ 2X Fast Q-PCR Master Mix (SYBR, no ROX; SMOBIO). All primers were designed using Primer3Plus (Table I). Additional reagents included agarose (Lonza), Tris-Acetate-EDTA buffer (Invitrogen), DNA markers (Vivantis), fetal bovine serum (FBS; Gibco), Fungizone (Gibco), MTT (Invitrogen), and HighGene Transfection Reagent (ABclonal).

Gene Design and DNA Cloning

Gene construction involved introducing *BglIII* (AGATCT) restriction enzyme sites, the ATG start codon, the *rE* gene, a TAATAA double stop codon, and the *EcoRI* (GAATTC) restriction enzyme site, which resulted in a 1,467-bp insert. The gene was then inserted into the multiple cloning site of the pEGFP-N1 vector. For transformation, *E. coli* DH5 α was cultured in LB broth medium at 150 rpm and 37°C for 16 h. Then, the *E. coli* DH5 α was subcultured in LB broth medium at 150 rpm for 3 h. Each subculture was transferred to a 1.5-mL tube and chilled on ice for 30 min. The subculture was centrifuged at 2,700 \times g at 4°C for 10 minutes. The supernatant was discarded, and the pellet containing *E. coli* DH5 α was resuspended in 1.5 mL of cold sterile 100 mM CaCl₂. The bacterial suspension in CaCl₂ was chilled on ice for 30 min, followed by centrifugation at 2,700 \times g for 10 min. The supernatant was discarded, and the pellet was resuspended again with 30 μ L of cold sterile 100 mM CaCl₂. The competent cells were incubated on ice for 2 h. Thereafter, DNA (10 ng/ μ L) was mixed with 30 μ L of competent cell suspension and incubated on ice for 30 min. A heat shock was applied by heating at 42°C for 45 s, followed by immediate chilling on ice for 2 min. The bacteria were added to 0.9 mL of LB broth medium and incubated at 37°C and 150 rpm for 90 min. The cells were subcultured on LB agar medium containing 50 μ g/mL of kanamycin for transformant selection.

Table I. Primer sequences used in the study

Primer code	Type	Sequence	Product size	Method
pEGFP-N1	Forward	5' TGGGAGGTCTATATAAGCAGAG 3'	1,648 bp	Sequencing
	Reverse	5' CGTCGCCGTCCAGCTCGACCAG 3'		
<i>rE</i> gene primer I	Forward	5' CGTTTAGCACCGAAGATGGT 3'	157 bp	Colony PCR
	Reverse	5' TTCAGGGCGTTATCACCAAT 3'		
<i>rE</i> gene primer II	Forward	5' ATAAGGAAATGGCCGAAACC 3'	134 bp	End-point RT-PCR and RT-qPCR
	Reverse	5' GCTAATAATACGGCCACCA 3'		
<i>GAPDH</i>	Forward	5' GAAGGTGAAGGTCCGAGTC 3'	226 bp	
	Reverse	5' GAAGATGGTGTATGGGATTTTC 3'		

Colony PCR and Recombinant Plasmid DNA Isolation

Transformed *E. coli* DH5 α carrying pEGFP-N1-*rE* was screened using colony PCR. A single colony was lightly picked with a sterile toothpick and directly transferred into the PCR reaction mix, which contained 0.5 μ L of each primer, 12.5 μ L of master mix, and 11.5 μ L of nuclease-free water. The PCR conditions were 95°C for 5 min, 25 cycles of 95°C for 30 s, 51°C for 30 s, and 72°C for 30 s, with a final extension at 72°C for 10 min. The products were confirmed by 1% agarose gel electrophoresis. Plasmid isolation was performed following the kit's protocol. The isolated recombinant plasmid was analyzed by 1% agarose gel electrophoresis and NanoDrop spectrophotometry (Maestro Gen).

PCR of Plasmid Isolation, Sequencing, and Data Analysis

PCR was performed using 2 μ L of the isolated plasmid, 1 μ L of each pEGFP-N1 primer, 25 μ L of master mix, and 21 μ L of nuclease-free water, following standard protocols. The 50 μ L PCR products were sent to Genetika Science for Sanger sequencing, and the results were analyzed using BioEdit.

Formulation of the DNA-Chitosan Complex

A 0.02% chitosan stock solution was prepared by dissolving 20 mg of medium-molecular-weight chitosan in 100 mL of 1% acetic acid. The solution's pH was modified to 5.0 by adding 1 M NaOH. The pEGFP-N1-*rE*/chitosan (N1-*rE*/CS) complex was formulated at DNA:chitosan mass ratios of 1:0.1, 1:0.2, 1:0.3, 1:0.4, and 1:0.5 (w/w), using 1000 ng of plasmid DNA for each formulation. These ratios were selected based on previous optimization studies for nucleic acid delivery (Kusumawati et al., 2024; Unsunnidhal et al., 2021), aiming to identify the minimum chitosan concentration that achieves complete DNA

encapsulation. The DNA and chitosan solutions were prepared and heated separately at 50°C for 10 min, combined in a 1:1 volume ratio, vortexed for 20 s, and incubated for 1 h. The formulations were analyzed by 0.8% agarose gel electrophoresis for 30 min at 100 V. Complete retardation (i.e., absence of free DNA bands) was considered indicative of optimal complexation.

DNA-Chitosan Complex Characterization

The particle size and zeta potential measurements were performed at the Faculty of Dentistry, Universitas Gadjah Mada, using a Zetasizer (Malvern Panalytical).

Stability Assay of the DNA-Chitosan Complex Against DNase I and FBS

The stability test against DNase I was performed by mixing and incubating 1 μ g of the nanoparticle complex, 20 μ L of DNase buffer, and 1 μ g of DNase I (1 U/mL) at 37°C for 30 min in a water bath. The FBS stability test was performed by mixing and incubating 1 μ g of the nanoparticle complex with 150 μ L of FBS at 37°C for 1 h in an incubator shaker.

MTT Cytotoxicity Assay

The cytotoxicity of the nanoparticle complex was assessed using the MTT assay. The complete medium was prepared by mixing 5 mL of FBS (10%), 1 mL of Penstrep (2%), and 250 μ L of Fungizone (0.5%) with RPMI to a final volume of 50 mL. HeLa cells (1×10^4 cells/100 μ L) were seeded in 96-well plates and incubated overnight at 37°C in 5% CO₂. Nanoparticle complexes (100 μ L) were added to each well and incubated for 24 h. After washing with 1 \times phosphate-buffered saline (PBS), 100 μ L of MTT (5 mg/mL) solution was added and incubated for 4 h at 37°C, followed by the addition of 100 μ L of 0.1 N SDS-HCl and overnight incubation at room temperature.

Optical density (OD) was measured at 550 nm using an ELISA reader. The OD of the cell-free medium was used to establish the background absorbance. Each experimental condition was plated in triplicate. Cell viability data were analyzed using one-way ANOVA, followed by Tukey's post hoc test. The cell viability (%) formula is as follows:

$$\text{Cell viability (\%)} = \frac{OD_{\text{treated cells}} - OD_{\text{medium}}}{OD_{\text{untreated cells}} - OD_{\text{medium}}} \times 100\%$$

Transfection of HeLa Cells with the N1-rE/CS Complex

Complete medium (10% FBS, 2% Penstrep, 0.5% Fungizone, and RPMI added to 50 mL) was prepared. HeLa cells (0.1×10^6 cells/well) were cultured in 12-well plates and incubated at 37°C under 95% humidity and 5% CO₂ conditions for 24 h. Transfection was performed when the cells reached 70%–80% confluency (0.5×10^6 cells/well) with five treatments: (1) non-transfected cells (negative control); transfected with (2) chitosan (negative control); (3) DNA (N1-rE, negative control); (4) DNA with HighGene Transfection Reagent (N1-rE/H, positive control); and (5) DNA-chitosan complex (N1-rE/CS). Each experimental condition was plated in triplicate. Two micrograms of DNA were added to each well, followed by a 4-h incubation, subsequent medium replacement, and incubation for a further 48 h.

Fluorescence Observation

Fluorescence imaging of protein expression in the transfected HeLa cells was performed using a ZEISS LSM 800 Confocal Microscope at 20× magnification. The cells were washed with PBS, fixed with cold methanol for 5 min, and rehydrated with PBS prior to imaging. Images were acquired from three fields of view within a single well. Image analysis was performed using ImageJ, and the corrected total cell fluorescence (CTCF) was calculated. CTCF values were compared using the Kruskal–Wallis test followed by Dunn's multiple comparisons test because of the non-normal data distribution and the unequal sample sizes from varying numbers of fluorescent cells per image. The CTCF formula is as follows:

$$\text{CTCF} = \text{integrated density} - (\text{area}_a \times \text{mean}_b)$$

a: selected cell b: fluorescence background

RNA Expression Analysis

Total RNA was isolated from HeLa cells using the Quick-RNA Miniprep Kit (Zymo Research). A 20-mg sample was mixed with 300 µL

RLT buffer in a 1.5 mL sterile tube and vortexed for 20–40 s. RNA isolation followed the kit protocol, and the isolated RNA was quantified using a NanoDrop spectrophotometer (Maestro Gen). The RNA isolates were stored at –80°C.

RNA expression was analyzed using end-point RT-PCR and qPCR, as previously described by I. L. Rahayu et al. (2019). For reverse transcription, 1 µg of RNA from HeLa cells was mixed with 1 µL of oligos (dT) and adjusted to 10 µL with DEPC-treated water. The mixture was incubated at 70°C for 5 min and immediately placed on ice for 1 min. The reaction was completed with 4 µL of 5X RT Buffer, 1 µL of RTase, and 5 µL of DEPC-treated water. Reverse transcription was performed at 25°C for 10 min, 45°C for 50 min, and 85°C for 5 min. The resulting cDNA was stored at –20°C. For end-point PCR, a mix of 1 µL of 10× diluted cDNA, 0.5 µL of each primer, 12.5 µL of master mix, and 10.5 µL of water was amplified according to the kit's protocol. The products were analyzed by 1.5% agarose gel electrophoresis. For qPCR, the reaction mix contained 1 µL of 10× diluted cDNA, 1 µL of each primer, 5 µL of qPCR master mix, and 2 µL of water. The qPCR was performed at 95°C for 2 min, with 40 cycles of 95°C for 15 s and 60°C for 30 s, followed by melting curve analysis. Each experimental condition for qPCR was performed in triplicate. Gene expression was analyzed using the 2^{–ΔΔCt} method (Livak & Schmittgen, 2001) and normalized to *GAPDH*. The normality of the ΔCt values was verified using the Shapiro–Wilk test. Statistical comparisons were performed between the groups using one-way ANOVA followed by Tukey's post hoc test. The relative gene expression was calculated as follows:

$$\begin{aligned} \Delta Ct_{\text{control}} &= Ct_{rE (\text{control})} - Ct_{GAPDH (\text{control})} \\ \Delta Ct_{\text{sample}} &= Ct_{rE (\text{sample})} - Ct_{GAPDH (\text{sample})} \\ \Delta Ct &= \Delta Ct_{\text{sample}} - \Delta Ct_{\text{control}} \\ \text{Relative expression} &= 2^{-\Delta\Delta Ct} \end{aligned}$$

RESULTS AND DISCUSSION

rE Gene Optimization

Codon optimization for mammalian expression improved the codon adaptation index (CAI) from 0.65 to 0.74. Rare codon analysis revealed a shift toward more frequently used codons, including a reduction in rarely used codons from 11% to 2%, which was crucial for enhanced protein expression (Faraji et al., 2017). In addition, the inclusion of the GCC codon alongside the ATG codon in the gene design forms the Kozak sequence, which is essential for translation initiation (Kozak, 1989).

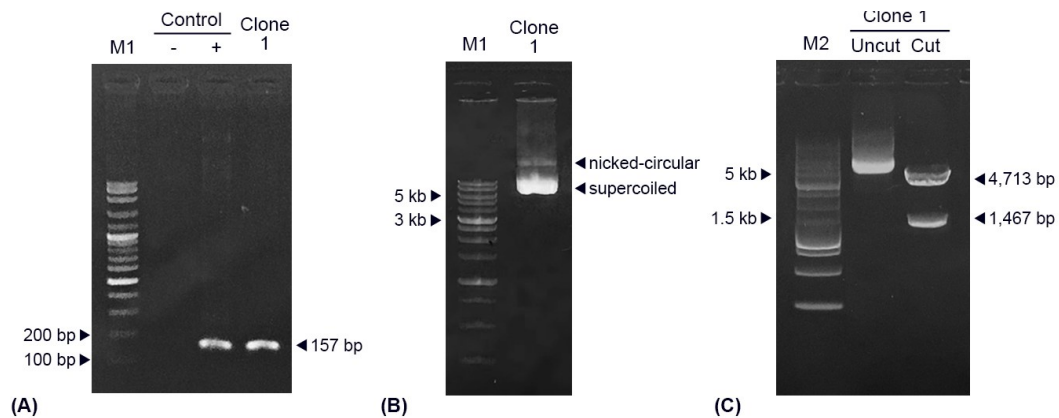


Figure 1. Verification of *Escherichia coli* DH5 α transformation with pEGFP-N1-*rE*. Transformed bacteria were selected on Luria-Bertani agar containing 50 μ g/mL kanamycin. (A) Colony PCR result confirming the presence of the *rE* gene in the transformed colony (Clone 1), non-transformed colony (Control -) and *rE* synthetic gene (Control +). (B) Agarose gel electrophoresis of the isolated N1-*rE* plasmid. (C) Restriction enzyme analysis of the undigested isolated plasmid (Uncut) and the digested isolated plasmid with *EcoRI* and *BglII* (Cut). M1=100 bp marker; M2=1,000 bp marker.

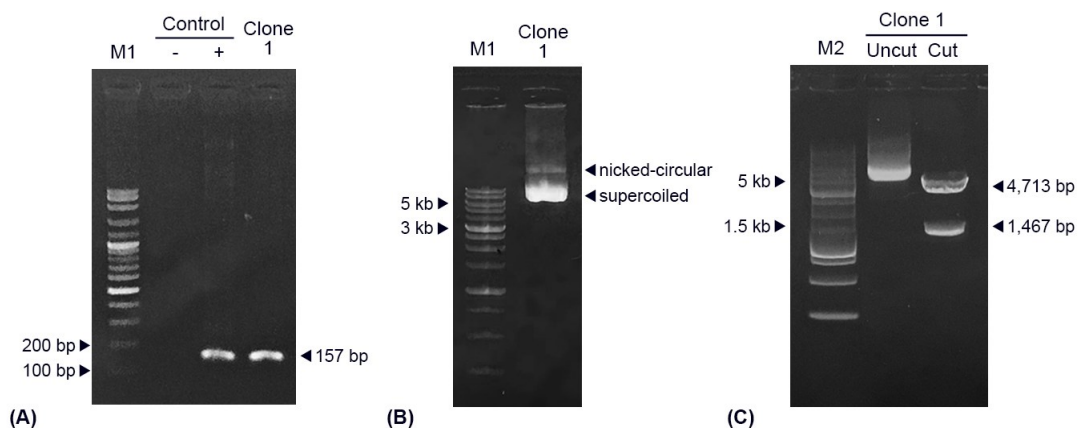


Figure 2. (A) Gel retardation assay results of the N1-*rE*/CS complex formulation with a DNA:chitosan mass ratio (w/w) of 1:0.1, 1:0.2, 1:0.3, 1:0.4, and 1:0.5. Negative controls included chitosan (CS) and the N1-*rE* plasmid (DNA). Results of the complex stability assays against (B) DNase I for 30 min and (C) fetal bovine serum (FBS) for 1 h. M = 1,000 bp marker.

As the GCC codon encodes alanine, a small and non-disruptive amino acid, it does not alter the conformation of the expressed *rE* protein (Unsunidhal et al., 2019).

Molecular diagnostics and sequencing analysis

Colony PCR confirmed the presence of the *rE* gene in the transformed colony (Figure 1A). Moreover, agarose gel electrophoresis after plasmid isolation revealed two conformations: nicked-circular and supercoiled bands (Figure 1B). The thicker supercoiled bands indicated high-quality plasmid isolation, as

supercoiled plasmids are intact, denser, and more stable (Smrek et al., 2021). Quantitative analysis revealed that the DNA was well-purified with a concentration of 2,223 ng/ μ L, an A260/A280 purity ratio of 1.870, and an A260/A230 ratio of 2.249. Restriction enzyme digestion with *BglII* and *EcoRI* yielded bands for the p-N1 backbone and *rE* gene (Figure 1C), thus verifying that the plasmid was correctly constructed and contained the desired genetic material. Sequencing analysis confirmed that no mutations occurred during plasmid cloning and isolation.

Formulation of the DNA-Chitosan Complex

The DNA-chitosan complex of the N1-*rE*/CS formulation was achieved using the complex coacervation method. The DNA:chitosan mass ratio was optimized based on previous studies and preliminary gel retardation assays. Gel retardation assays revealed that two distinct bands were observed at lower chitosan:DNA mass ratios (1:0.1 to 1:0.4): one corresponding to the DNA-chitosan complex trapped in the well and another for free unencapsulated DNA migrating through the gel (Figure 2A). As the chitosan mass increased, more DNA was encapsulated within the complex, thus reducing the amount of free DNA that could migrate through the gel. Consequently, this resulted in a single band in the well. The optimal ratio of 1:0.5 effectively captured the entire plasmid DNA and was used for subsequent assays. Previous studies have reported various optimal ratios for DNA-chitosan complexes. Kusumawati et al. (2024) found a 1:0.6 ratio was optimal for *S1* gene delivery using pEGFP-N1, which closely aligns with our findings, while Unsunnidhal et al. (2021) reported a 1:2 ratio for the optimal delivery of the *tat* gene using pcDNA3.1. These variations are likely due to differences in the plasmid choice, DNA sequence, and other formulation parameters. Notably, these three studies used chitosan with similar molecular weight and degree of deacetylation, indicating that the plasmid sequence composition likely plays a pivotal role in determining the optimal ratio. Specifically, GC-rich regions, which are more kinetically constrained, tend to facilitate easier condensation with chitosan (Y. Yang et al., 2017). Although increasing the chitosan mass improves DNA binding, it may also result in larger particle sizes and aggregation, thereby potentially impairing cellular uptake and transfection efficiency (Pilipenko et al., 2019).

The formation of the nanoparticle complex is caused by the electrostatic interactions between chitosan and DNA. Under acidic pH conditions, the primary amino groups of chitosan become protonated, causing chitosan to gain a more positive charge. Conversely, DNA is negatively charged. This condition creates a charge disparity between them and allows for the spontaneous self-assembly into a stable complex (Wang et al., 2015).

Stability Against DNase I and FBS

The stability of the N1-*rE*/CS complex against nuclease degradation was evaluated using DNase I and FBS. While the naked N1-*rE* plasmid was completely degraded, intact bands of the N1-

rE/CS complex remained visible following DNase I treatment (1 U/ μ L for 30 min) and incubation with 33.3% (v/v) FBS for 1 h at 37°C (Figure 2B and 2C). These results may indicate the protective role of chitosan against DNA degradation. Huang et al. (2005) found similar results in a DNase I assay, and this was attributed to the steric hindrance provided by the positive charge of chitosan that prevents nuclease access to the DNA. In addition to assessing the complex stability under high DNase I concentrations, intact bands of the complex following incubation with FBS may provide further insights into the complex stability for in vitro applications. FBS is commonly used for cell supplementation in in vitro systems and has been reported to interfere with nucleic acid expression because of its nuclease content (Hahn et al., 2014). Moreover, in vivo applications must also contend with nuclease activity in bodily fluids, including serum. Many types of serum, such as those from humans, mice, and fetal bovines, were found to contain various nucleases, including DNase I, DNase1L3 (Lauková et al., 2020), lactoferrin, and DNA-hydrolyzing autoantibodies (Vancevska & Nikolic, 2013).

Cytotoxicity Analysis of the DNA-Chitosan Complex

An MTT assay was performed to assess the potential toxicity of the N1-*rE*/CS complex delivery system in HeLa cells prior to transfection. By measuring the reduction of the tetrazolium ring of MTT to formazan crystals by mitochondrial dehydrogenases, which can only be performed by living cells, the MTT assay can estimate the cytotoxicity of a tested compound (Boyras et al., 2021). The N1-*rE*/CS treatment exhibited 91.24% cell viability, and the other treatments demonstrated similar viability (Figure 3). According to Gomes-Cornélio et al. (2017), a minimum cell viability of 80% is potentially indicative of the non-cytotoxicity of a compound, which suggests that N1-*rE*/CS is a nontoxic complex. However, when the cell viability of N1-*rE*/CS was statistically analyzed further, it was considered a significant reduction ($p = 0.03$) compared with that of the control. This suggests that while N1-*rE*/CS may exhibit characteristics of a relatively safe delivery platform, it does exhibit a minor cytotoxic effect at the tested concentration (1 μ g/mL), but the overall impact on cell health is possibly not sufficient to be considered harmful. Further optimization may be required to reduce residual cytotoxicity.

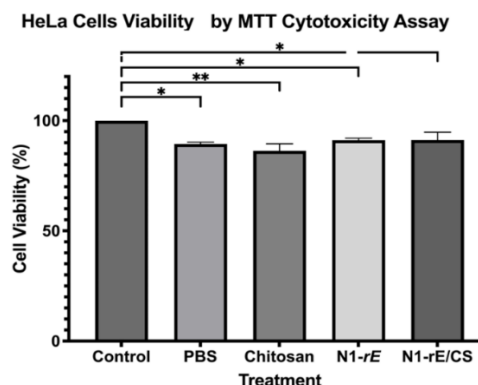


Figure 3. Results of the MTT cytotoxicity assay in HeLa cells treated with chitosan, phosphate-buffered saline (PBS), N1-rE, and N1-rE/CS at a concentration of 1 $\mu\text{g}/\text{mL}$. Bars represent the mean ($n=3$) \pm standard deviation. Significance: * $P < 0.05$; ** $P < 0.01$.

Chitosan degradation involves the depolymerization of β -1,4-glycosidic bonds, followed by deacetylation, with factors such as the molecular weight and degree of deacetylation affecting the process (Matica et al., 2017). This process primarily occurs via lysozymes. Generally, chitosan is reported to have low toxicity, with an IC_{50} of 0.2–2.5 mg/mL in cell models (Kean & Thanou, 2010), although modifications may alter its toxicity profile. The FDA has approved the use of chitosan for several applications, including hemostatic dressings and contact lens coating. Furthermore, chitosan is considered a Generally Recognized as Safe food additive. That said, chitosan-based delivery systems remain mostly experimental, as none have received regulatory approval to date (Suryani et al., 2024).

Gene Expression of Chitosan-Mediated DNA Delivery

This study employed the pEGFP-N1 vector, with the *rE* gene inserted between the *Bgl*II and *Eco*RI restriction enzyme sites, producing a fusion protein rE-EGFP. EGFP serves as a fluorescent marker that emits green fluorescence under blue to ultraviolet light, thereby allowing the detection of rE expression via confocal microscopy (Figure 4A). Bright-field observations of HeLa cells revealed healthy cell morphologies across all treatments, characterized by a predominance of confluent, irregularly shaped attached cells with cytoplasmic projections (Ekowati et al., 2017; Maruti et al., 2017). Moreover, confocal microscopy showed that green fluorescence was observed in cells treated

with the *rE* gene delivered by HighGene (N1-rE/H) and chitosan (N1-rE/CS). These findings align with the studies by Maulina et al. (2023) and Unsunnidhal et al. (2019), which reported similar results in HeLa cells transfected with pEGFP-*rE* using Lipofectamine™ 3000 and *gag-CA* using chitosan, respectively. Furthermore, image analysis with CTCF quantification (Figure 4B) confirmed that the N1-rE/H treatment exhibited the highest fluorescence intensity (2.10×10^4 a.u.), followed by N1-rE/CS (8.91×10^3 a.u.), both demonstrating significant differences compared to those of the untreated controls. Due to the non-normal data distribution and unequal sample sizes, the Kruskal-Wallis test with Dunn's test post hoc was used as a nonparametric statistical approach. This choice accounts for the naturally stochastic variability of transient transfection, which can lead to substantial differences in gene expression between individual cells (Wang et al., 2018).

The isolated RNA samples underwent a two-step RT-PCR to evaluate their expression levels. End-point RT-PCR confirmed a 134-bp amplification product for the *rE* gene in N1-rE/CS-treated cells (Figure 5A). Negative results were obtained for the untreated HeLa cells as well as those treated with chitosan alone and N1-rE. Moreover, expression analysis was conducted using quantitative PCR (Figure 5B). The N1-rE/CS treatment showed a 10.63-fold increase in *rE* gene expression compared with that of N1-rE (naked DNA). However, the expression was lower than the 363.72-fold increase observed with HighGene (N1-rE/H), a commercial transfection reagent. To ensure accurate statistical analysis, ΔCt values were used instead of the fold change. The subtraction of the reference gene Ct in the ΔCt calculations preserves data linearity, unlike the exponential transformation in fold change, which can introduce skewed distributions (Billard et al., 2014). Normality testing confirmed that the ΔCt values were normally distributed across all groups. One-way ANOVA and Tukey's post hoc test further confirmed that N1-rE/CS exhibited a significant increase ($P = 0.0002$) in expression compared with that of N1-rE, while N1-rE/H exhibited a significantly higher expression ($P < 0.0001$) than that of N1-rE (Figure 5C). These findings align with previous studies reporting lower transfection efficiency for chitosan-based delivery compared with commercial transfection reagents such as Lipofectamine™ 3000 (Unsunidhal et al., 2019) and TransIntro™ EL Transfection Reagent (Rahayu et al., 2019).

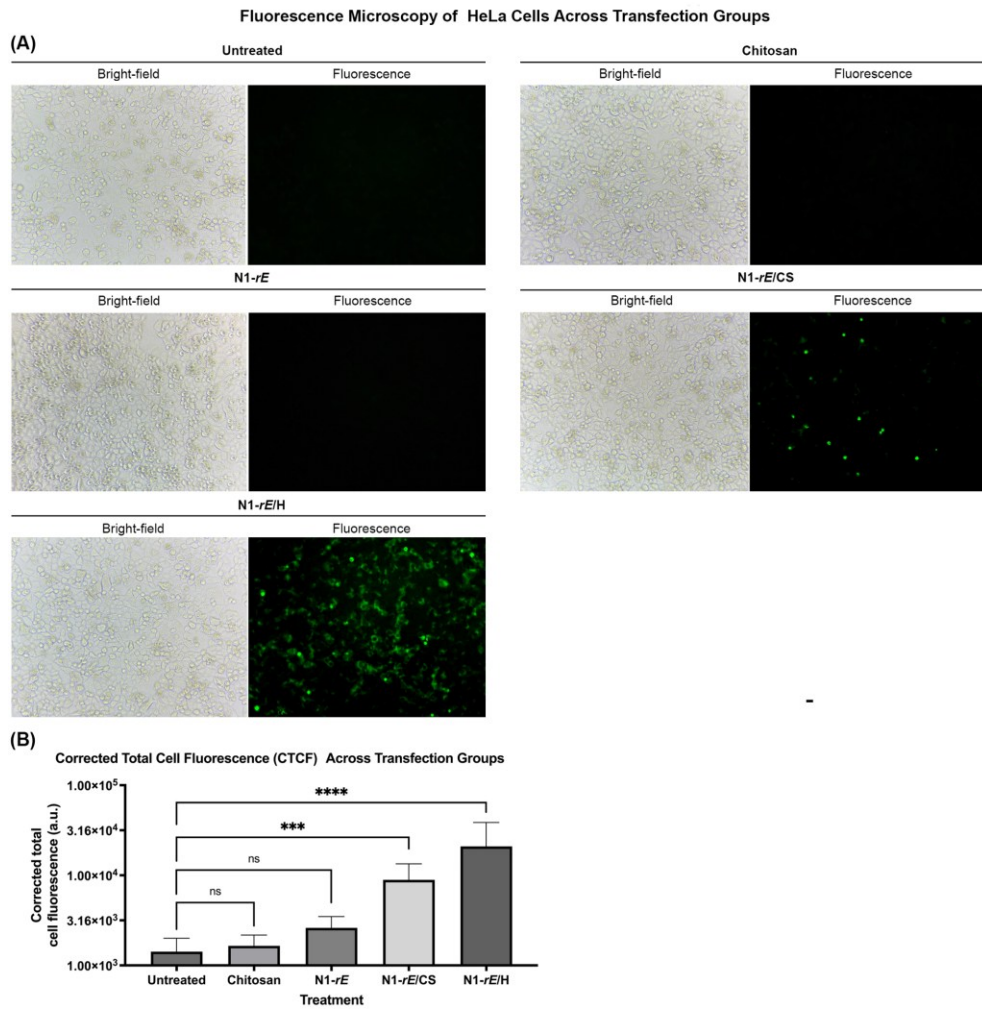


Figure 4. (A) Bright-field and fluorescence images (20×) of HeLa cells from the untreated, chitosan, N1-rE, N1-rE/H, and N1-rE/CS groups. Green fluorescence shows protein expression. (B) Corrected total cell fluorescence (CTCF) quantification. Bars represent the mean ± standard deviation. Kruskal–Wallis with Dunn’s test was used because of the unequal sample sizes. Significance: P > 0.05, ***P < 0.001, ****P < 0.0001.

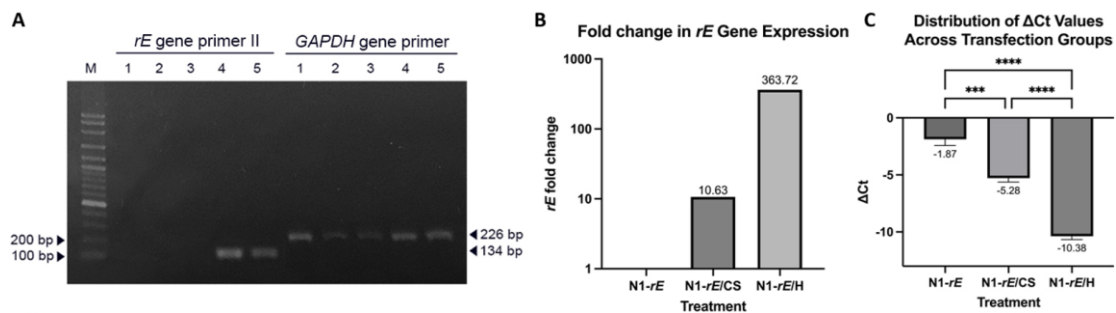


Figure 5. Gene expression analysis using end-point RT-PCR and qPCR. (A) End-point RT-PCR amplification of rE (134 bp) and GAPDH (226 bp) in the mRNA samples from (1) untreated HeLa cells, (2) chitosan, (3) N1-rE, (4) N1-rE/H, and (5) N1-rE/CS. M=100 bp marker. (B) qPCR analysis of the relative rE gene expression levels in HeLa cells transfected with chitosan (N1-rE/CS) and HighGene (N1-rE/H) delivery systems. (C) Distribution of ΔCt values across the control (N1-rE), N1-rE/CS, and N1-rE/H groups. Bars represent the mean (n=3) ± standard deviation. Significance: ***P < 0.001; ****P < 0.0001.

The stark contrast in the fold change between N1-*rE*/H (363.72-fold increase) and N1-*rE*/CS (10.63-fold increase) reflects variations in the transfection efficiency, DNA release kinetics, and endosomal escape capability. The superior efficiency of HighGene is likely due to enhanced endosomal escape and the rapid intracellular DNA release (Cai et al., 2023; Wang et al., 2023). In contrast, chitosan-mediated delivery is influenced by its pH-dependent buffering capacity, which may limit effective endosomal escape, resulting in a slower intracellular plasmid release (Fidan et al., 2024). The release process follows a biphasic pattern, which is characterized by a rapid phase during the first 3 h, followed by a sustained release extending up to 72 h (Ishak et al., 2019). Notably, while the expression increased with N1-*rE*/CS was lower than that of the commercial reagent, the transfection thereof was significantly improved compared to that of naked DNA, which is prone to nuclease degradation and ineffective expression.

Complex Characteristics and Their Relevance in Gene Delivery and Expression

The zeta potential reflects the complex surface charge, which influences the colloidal stability and cellular interactions. Highly positive or negative values promote stability by preventing aggregation through electrostatic repulsion (Sabbah & Esposito, 2016). The N1-*rE*/CS complex had a zeta potential of -21.9 mV, falling within the ± 20 – 30 mV range, indicating that it forms a moderately stable colloid (Ardani et al., 2017). While zeta potentials exceeding ± 30 mV generally enhance stability, the observed value provides sufficient repulsion to prevent aggregation (Honary & Zahir, 2013). DNA-chitosan complexes have been shown to retain stability for at least 72 h (Raimbekova et al., 2025). Separately, formulations prepared at pH 5.5 have demonstrated consistent zeta potential and particle size over 3 months, indicating that the DNA-chitosan complex exhibits good physicochemical stability during storage (Bozkir & Saka, 2004). Moreover, the negative zeta potential of N1-*rE*/CS may hinder electrostatic interactions with the negatively charged cell membrane, thus potentially slowing uptake and reducing efficiency (Németh et al., 2022). However, while the positively charged nanoparticles enhance cellular uptake, they also pose a higher risk of cytotoxicity by disrupting the plasma membrane, which makes chitosan's lower but sustained transfection a potential advantage (Bannunah et al., 2014).

The DNA-chitosan complex transfection efficiency can also be influenced by the particle size. Particle size analysis showed that the N1-*rE*/CS nanoparticles ranged from 100 to 300 nm, with an average size of 217.4 nm. This aligns with studies where 230 kDa chitosan formed ~ 300 nm nanoparticles (MacLaughlin et al., 1998), which suggests that the 190–310 kDa chitosan used in this study contributed to the observed nanoparticle size. Nanoparticle size is a critical factor in determining how efficiently it enters a cell, likely because of the available surface area for membrane interactions (Seleci et al., 2016). This principle is well illustrated by DNA-chitosan complexes; for example, particles approximately 200 nm in size consistently exhibit higher transfection efficiency than 400 nm complexes (Poor et al., 2014). Apirakaramwong et al. (2012) suggested that DNA-chitosan complexes are primarily taken up via caveolae-mediated endocytosis, with clathrin-dependent routes serving as a secondary mechanism, although the exact particle size was not specified. This is noteworthy, as the caveolae pathway, while potentially slower, provides the advantage of bypassing degradation in the lysosome and possibly allowing a more direct route to the nucleus (Yang et al., 2021). These pathways typically accommodate particles smaller than 200 nm, whereas larger particles are more likely to be internalized via macropinocytosis (Rennick et al., 2021). This creates an interpretive picture for our study, which has a particle size distribution of 100–300 nm. It seems probable that these multiple pathways govern the uptake of the nanoparticle complex. However, the route is probably not fixed and shifts in response to the particle size, surface characteristics, and dynamic behavior of the cell membrane.

Limitations and Future Perspectives

Our findings regarding chitosan as a gene delivery vehicle are encouraging; however, several limitations must be recognized that delineate the boundaries of our conclusions. For example, the transfection efficiency was not as high as that with the commercial reagents. This difference might likely be due to challenges such as poor endosomal escape. In future studies, several methods that have previously been demonstrated to increase cellular entry and therefore gene expression, such as quaternization, PEGylation, or the conjugation of particular ligands, could be investigated further (Cao et al., 2019). In addition, we did not use direct protein analyses, such as SDS-PAGE and western

blotting, which would have clarified the downstream functional results of transfection. Our research was also limited to HeLa cells, a model system that might not accurately predict performance under different cellular conditions or tissue settings. Furthermore, in vivo studies could be conducted to assess the immunogenicity, biodistribution, and sustained gene expression of the chitosan delivery system.

CONCLUSION

The optimum complex formation between the recombinant plasmid N1-*rE* and chitosan was obtained at a DNA:chitosan mass ratio of 1:0.5 (w/w), as evidenced by the gel retardation assay. Moreover, fluorescence observation, end-point RT-PCR, and qPCR verified that this complex promoted *rE* gene expression in HeLa cells. These results demonstrate the potential of chitosan nanoparticles as a viable platform for the development of a DNA vaccine against DENV infection.

ACKNOWLEDGMENTS

The authors would like to acknowledge Universitas Gadjah Mada for providing the essential facilities and resources that made this research possible.

CONFLICT OF INTEREST

The authors declare no conflict of interest.

REFERENCES

- Alves, A. M. B., Costa, S. M., & Pinto, P. B. A. (2021). Dengue virus and vaccines: how can DNA immunization contribute to this challenge? *Frontiers in Medical Technology*, 3. <https://doi.org/10.3389/fmedt.2021.640964>
- Apirakaramwong, A., Pamonsinlapatham, P., Techaarpornkul, S., Opanasopit, P., Panomsuk, S., & Soksawatmaekhin, S. (2012). Mechanisms of cellular uptake with chitosan/DNA complex in hepatoma cell line. *Advanced Materials Research*, 506, 485–488. <https://doi.org/10.4028/www.scientific.net/AMR.506.485>
- Ardani, H. K., Imawan, C., Handayani, W., Djuhana, D., Harmoko, A., & Fauzia, V. (2017). Enhancement of the stability of silver nanoparticles synthesized using aqueous extract of *Diospyros discolor* Willd. leaves using polyvinyl alcohol. *IOP Conference Series: Materials Science and Engineering*, 188, 012056. <https://doi.org/10.1088/1757-899X/188/1/012056>
- Asyura, M. M. A. Z., Fauzi, A., & Ayub, F. A. (2021). Potential of peptide-based non-structural protein 1 (NS1) inhibitor in obstructing dengue virus (DENV) replication. *Green Medical Journal*, 3(1), 1–12. <https://doi.org/10.33096/gmj.v3i1.71>
- Bannunah, A. M., Vllasaliu, D., Lord, J., & Stolnik, S. (2014). Mechanisms of nanoparticle internalization and transport across an intestinal epithelial cell model: effect of size and surface charge. *Molecular Pharmaceutics*, 11(12), 4363–4373. <https://doi.org/10.1021/mp500439c>
- Billard, V., Ourry, A., Maillard, A., Garnica, M., Coquet, L., Jouenne, T., Cruz, F., Garcia-Mina, J.-M., Yvin, J.-C., & Etienne, P. (2014). Copper-deficiency in *Brassica napus* induces copper remobilization, molybdenum accumulation and modification of the expression of chloroplastic proteins. *PLoS ONE*, 9(10), e109889. <https://doi.org/10.1371/journal.pone.0109889>
- Boyraz, M. Ü., Shekhany, B., & Süzergöz, F. (2021). Cellular imaging analysis of MTT assay based on tetrazolium reduction. *Harran Üniversitesi Tıp Fakültesi Dergisi*, 18(1), 95–99. <https://doi.org/10.35440/hutfd.816390>
- Bozkir, A., & Saka, O. M. (2004). Chitosan–DNA nanoparticles: effect on DNA integrity, bacterial transformation and transfection efficiency. *Journal of Drug Targeting*, 12(5), 281–288. <https://doi.org/10.1080/10611860410001714162>
- Cai, X., Dou, R., Guo, C., Tang, J., Li, X., Chen, J., & Zhang, J. (2023). Cationic polymers as transfection reagents for nucleic acid delivery. *Pharmaceutics*, 15(5), 1502. <https://doi.org/10.3390/pharmaceutics15051502>
- Cao, Y., Tan, Y. F., Wong, Y. S., Liew, M. W. J., & Venkatraman, S. (2019). Recent advances in chitosan-based carriers for gene delivery. *Marine Drugs*, 17(6), 381. <https://doi.org/10.3390/md17060381>
- Ekowati, N., Mumpuni, A., & Muljowati, J. S. (2017). Effectiveness of *Pleurotus ostreatus* extract through cytotoxic test and apoptosis mechanism of cervical cancer cells.

- Biosaintifika: Journal of Biology & Biology Education*, 9(1), 148.
<https://doi.org/10.15294/biosaintifika.v9i1.17546>
- Fahimi, H., Sadeghzadeh, M., & Mohammadipour, M. (2016). In silico analysis of an envelope domain III-based multivalent fusion protein as a potential dengue vaccine candidate. *Clinical and Experimental Vaccine Research*, 5(1), 41.
<https://doi.org/10.7774/cevr.2016.5.1.41>
- Faraji, H., Ramezani, M., Sadeghnia, H. R., Abnous, K., Soltani, F., & Mashkani, B. (2017). High-level expression of a biologically active staphylokinase in *Pichia pastoris*. *Preparative Biochemistry & Biotechnology*, 47(4), 379–387.
<https://doi.org/10.1080/10826068.2016.1252924>
- Fidan, E. B. E., Bal, K., Şentürk, S., Kaplan, Ö., Demir, K., & Gök, M. K. (2024). Enhancing gene delivery efficiency with amphiphilic chitosan modified by myristic acid and tertiary amino groups. *International Journal of Biological Macromolecules*, 282, 136775.
<https://doi.org/10.1016/j.ijbiomac.2024.136775>
- Gomes-Cornélio, A. L., Rodrigues, E. M., Salles, L. P., Mestieri, L. B., Faria, G., Guerreiro-Tanomaru, J. M., & Tanomaru-Filho, M. (2017). Bioactivity of MTA Plus, Biodentine and an experimental calcium silicate-based cement on human osteoblast-like cells. *International Endodontic Journal*, 50(1), 39–47.
<https://doi.org/10.1111/iej.12589>
- Hahn, J., Wickham, S. F. J., Shih, W. M., & Perrault, S. D. (2014). Addressing the instability of DNA nanostructures in tissue culture. *ACS Nano*, 8(9), 8765–8775.
<https://doi.org/10.1021/nn503513p>
- Halstead, S. B. (2024). Three dengue vaccines — what now? *New England Journal of Medicine*, 390(5), 464–465.
<https://doi.org/10.1056/NEJMe2314240>
- Honary, S., & Zahir, F. (2013). Effect of zeta potential on the properties of nano-drug delivery systems - a review (part 2). *Tropical Journal of Pharmaceutical Research*, 12(2).
<https://doi.org/10.4314/tjpr.v12i2.20>
- Huang, M., Fong, C.-W., Khor, E., & Lim, L.-Y. (2005). Transfection efficiency of chitosan vectors: Effect of polymer molecular weight and degree of deacetylation. *Journal of Controlled Release*, 106(3), 391–406.
<https://doi.org/10.1016/j.jconrel.2005.05.004>
- Ishak, J., Unsunnidhal, L., Martien, R., & Kusumawati, A. (2019). In vitro evaluation of chitosan-DNA plasmid complex encoding jembrana disease virus Env-TM protein as a vaccine candidate. *Journal of Veterinary Research*, 63(1), 7–16.
<https://doi.org/10.2478/jvetres-2019-0018>
- Kaur, M., Sharma, A., Puri, V., Aggarwal, G., Maman, P., Huanbutta, K., Nagpal, M., & Sangnim, T. (2023). Chitosan-based polymer blends for drug delivery systems. *Polymers*, 15(9), 2028.
<https://doi.org/10.3390/polym15092028>
- Kean, T., & Thanou, M. (2010). Biodegradation, biodistribution and toxicity of chitosan. *Advanced Drug Delivery Reviews*, 62(1), 3–11.
<https://doi.org/10.1016/j.addr.2009.09.004>
- Kozak, M. (1989). The scanning model for translation: an update. *The Journal of Cell Biology*, 108(2), 229–241.
<https://doi.org/10.1083/jcb.108.2.229>
- Kusumawati, A., Fahlevi, N. A., Pratiwi, R., Jannah, R., & Maulina, N. T. A. (2024). Chitosan potential as delivery agent for S1 gene from SARS-CoV-2 with pEGFP-N1 as its vectors. *Journal of Health (JoH)*, 11(02), 119–127.
<https://doi.org/10.30590/joh.v11n2.716>
- Lai, S.-C., Huang, Y.-Y., Shu, P.-Y., Chang, S.-F., Hsieh, P.-S., Wey, J.-J., Tsai, M.-H., Ben, R.-J., Hsu, Y.-M., Fang, Y.-C., Hsiao, M.-L., & Lin, C.-C. (2019). Development of an enzyme-linked immunosorbent assay for rapid detection of dengue virus (DENV) NS1 and differentiation of DENV serotypes during early infection. *Journal of Clinical Microbiology*, 57(7).
<https://doi.org/10.1128/JCM.00221-19>
- Lauková, L., Konečná, B., Janovičová, L., Vlková, B., & Celec, P. (2020). Deoxyribonucleases and their applications in biomedicine. *Biomolecules*, 10(7), 1036.
<https://doi.org/10.3390/biom10071036>
- Livak, K. J., & Schmittgen, T. D. (2001). Analysis of relative gene expression data using real-time quantitative PCR and the 2- $\Delta\Delta$ CT method. *Methods*, 25(4), 402–408.
<https://doi.org/10.1006/meth.2001.1262>
- MacLaughlin, F. C., Mumper, R. J., Wang, J., Tagliaferri, J. M., Gill, I., Hinchcliffe, M., &

- Rolland, A. P. (1998). Chitosan and depolymerized chitosan oligomers as condensing carriers for in vivo plasmid delivery. *Journal of Controlled Release*, 56(1–3), 259–272. [https://doi.org/10.1016/S0168-3659\(98\)00097-2](https://doi.org/10.1016/S0168-3659(98)00097-2)
- Maruti, A. A., Amalia, F., & Meiyanto, E. (2017). Synergistic effect of arecoline in combination with doxorubicin on HeLa cervical cancer cells. *Indonesian Journal of Cancer Chemoprevention*, 6(2), 64. <https://doi.org/10.14499/indonesianjancanchemoprev6iss2pp64-70>
- Matica, A., Menghiu, G., & Ostafe, V. (2017). Biodegradability of chitosan based products. *New Frontiers in Chemistry*, 26(1), 75–86.
- Maulina, N. T. A., Kusumawati, A., & Umniyati, S. R. (2023). *Ekspresi gen rE virus dengue pada sel HeLa menggunakan vektor pEGFP-N1 [Expression of the dengue virus rE gene in HeLa cells using the pEGFP-N1 vector]* [Master's thesis, Universitas Gadjah Mada]. <https://etd.repository.ugm.ac.id/penelitian/detail/221230>
- Németh, Z., Csóka, I., Semnani Jazani, R., Sipos, B., Haspel, H., Kozma, G., Kónya, Z., & Dobó, D. G. (2022). Quality by design-driven zeta potential optimisation study of liposomes with charge imparting membrane additives. *Pharmaceutics*, 14(9), 1798. <https://doi.org/10.3390/pharmaceutics14091798>
- Pilipenko, I., Korzhikov-Vlakh, V., Sharoyko, V., Zhang, N., Schäfer-Korting, M., Rühl, E., Zoschke, C., & Tennikova, T. (2019). pH-sensitive chitosan–heparin nanoparticles for effective delivery of genetic drugs into epithelial cells. *Pharmaceutics*, 11(7), 317. <https://doi.org/10.3390/pharmaceutics11070317>
- Poor, E. M., Baghaban Eslaminejad, M., Gheibi, N., Bagheri, F., & Atyabi, F. (2014). Chitosan–pDNA nanoparticle characteristics determine the transfection efficacy of gene delivery to human mesenchymal stem cells. *Artificial Cells, Nanomedicine, and Biotechnology*, 42(6), 376–384. <https://doi.org/10.3109/21691401.2013.832685>
- Rahayu, A., Saraswati, U., Supriyati, E., Kumalawati, D. A., Hermantara, R., Rovik, A., Daniwijaya, E. W., Fitriana, I., Setyawan, S., Ahmad, R. A., Wardana, D. S., Indriani, C., Utarini, A., Tantowijoyo, W., & Arguni, E. (2019). Prevalence and distribution of dengue virus in *Aedes aegypti* in Yogyakarta City before deployment of *Wolbachia* infected *Aedes aegypti*. *International Journal of Environmental Research and Public Health*, 16(10), 1742. <https://doi.org/10.3390/ijerph16101742>
- Rahayu, I. L., Kusumawati, A., & Martien, R. (2019). *Optimasi formula kandidat vaksin DNA (env-Tm) penyakit demam berdarah berbasis kitosan dan poly(D-L-Lactic co-glicolide acid) [Optimization of the DNA vaccine candidate formula (env-Tm) for dengue disease based on chitosan and poly(D,L-lactic co-glycolic acid)]* [Master's thesis, Universitas Gadjah Mada]. <https://etd.repository.ugm.ac.id/penelitian/detail/182121>
- Raimbekova, A., Kart, U., Yerishova, A., Elebessov, T., Yegorov, S., Pham, T. T., & Hortelano, G. (2025). Chitosan-DNA nanoparticles: synthesis and optimization for long-term storage and effective delivery. *PeerJ*, 13, e18750. <https://doi.org/10.7717/peerj.18750>
- Rennick, J. J., Johnston, A. P. R., & Parton, R. G. (2021). Key principles and methods for studying the endocytosis of biological and nanoparticle therapeutics. *Nature Nanotechnology*, 16(3), 266–276. <https://doi.org/10.1038/s41565-021-00858-8>
- Sabbah, M., & Esposito, M. (2016). Insight into zeta potential measurements in biopolymer film preparation. *Journal of Biotechnology & Biomaterials*, 6(2). <https://doi.org/10.4172/2155-952X.1000e126>
- Santos-Carballal, B., Fernández Fernández, E., & Goycoolea, F. (2018). Chitosan in non-viral gene delivery: role of structure, characterization methods, and insights in cancer and rare diseases therapies. *Polymers*, 10(4), 444. <https://doi.org/10.3390/polym10040444>
- Seleci, M., Ag Seleci, D., Jonczyk, R., Stahl, F., Blume, C., & Scheper, T. (2016). Smart multifunctional nanoparticles in nanomedicine. *BioNanoMaterials*, 17(1–2), 33–41. <https://doi.org/10.1515/bnm-2015-0030>
- Srinivas, K. P. (2021). Recent developments in vaccines strategies against human viral

- pathogens. In *Recent Developments in Applied Microbiology and Biochemistry* (pp. 3–12). Elsevier. <https://doi.org/10.1016/B978-0-12-821406-0.00001-1>
- Suryani, S., Chaerunisaa, A., Joni, I. M., Ruslin, R., Aspadih, V., Anton, A., Sartinah, A., & Ramadhan, L. O. A. (2024). The chemical modification to improve solubility of chitosan and its derivatives application, preparation method, toxicity as a nanoparticles. *Nanotechnology, Science and Applications, Volume 17*, 41–57. <https://doi.org/10.2147/NSA.S450026>
- Tarigan, M. (2025, April 27). Masyarakat masih anggap ringan penyakit DBD, padahal bisa sebabkan kematian [Public still underestimates dengue fever, despite its potential to cause death]. *Tempo*. <https://www.tempo.co/gaya-hidup/masyarakat-masih-anggap-ringan-penyakit-dbd-padahal-bisa-sebabkan-kematian-1267326>
- Unsunidhal, L., Ishak, J., & Kusumawati, A. (2019). Expression of gag-CA gene of jembrana disease virus with cationic liposomal and chitosan nanoparticle delivery systems as DNA vaccine candidates. *Tropical Life Sciences Research, 30*(3), 15–36. <https://doi.org/10.21315/tlsr2019.30.3.2>
- Unsunidhal, L., Wasito, R., Nugraha Setyawan, E. M., & Kusumawati, A. (2021). Potential of nanoparticles chitosan for delivery pcDNA3.1-tat. *BIO Web of Conferences, 41*, 07004. <https://doi.org/10.1051/bioconf/20214107004>
- Vancevska, A., & Nikolic, A. (2013). Assessment of deoxyribonuclease activity in biological samples by a fluorescence detection-based method. *Laboratory Medicine, 44*(2), 125–128. <https://doi.org/10.1309/LMD9INNMFDO5XGIW>
- Wang, J., Isaacson, S. A., & Belta, C. (2018). Predictions of genetic circuit behaviors based on modular composition in transiently transfected mammalian cells. *2018 IEEE Life Sciences Conference (LSC)*, 85–88. <https://doi.org/10.1109/LSC.2018.8572174>
- Wang, R., Huang, Y., Gan, X., Fu, C., Li, Y., Chen, N., Xi, H., Guo, H., Zhang, W., Lü, Y., Zhang, Y., & Lü, P. (2023). Switch of phosphorylation to O-GlcNAcylation of AhR contributes to vascular oxidative stress induced by benzo[a]pyrene. *Food Science and Human Wellness, 12*(6), 2263–2275. <https://doi.org/10.1016/j.fshw.2023.03.046>
- Wang, Y., Zhang, X., & Yang, G. (2015). Single molecular analysis of the interaction between DNA and chitosan. *RSC Advances, 5*(37), 29594–29600. <https://doi.org/10.1039/C4RA15612A>
- World Health Organization. (2024, April 23). *Dengue and severe dengue*. World Health Organization. <https://www.who.int/news-room/fact-sheets/detail/dengue-and-severe-dengue>
- Yang, C., He, B., Dai, W., Zhang, H., Zheng, Y., Wang, X., & Zhang, Q. (2021). The role of caveolin-1 in the biofate and efficacy of anti-tumor drugs and their nano-drug delivery systems. *Acta Pharmaceutica Sinica B, 11*(4), 961–977. <https://doi.org/10.1016/j.apsb.2020.11.020>
- Yang, Y., Guo, M., Qian, R., Liu, C., Zong, X., Li, Y.-Q., & Li, W. (2017). Binding efficacy and kinetics of chitosan with DNA duplex: the effects of deacetylation degree and nucleotide sequences. *Carbohydrate Polymers, 169*, 451–457. <https://doi.org/10.1016/j.carbpol.2017.04.040>